# Fuel Minimization of Plug-in Hybrid Electric Vehicles by Optimizing Drive Mode Selection

Chi-Kin Chau
Masdar Institute of Science and Technology
ckchau@masdar.ac.ae

Khaled Elbassioni
Masdar Institute of Science and Technology
kelbassioni@masdar.ac.ae

Chien-Ming Tseng
Masdar Institute of Science and Technology
ctseng@masdar.ac.ae

## ABSTRACT

Plug-in hybrid electric vehicles (PHEVs) are a viable energy-efficient means of transportation, which enjoy both convenience of fuel refilling and cheap electrical energy. But PHEVs have complex dynamics of orchestrating hybrid energy sources. While many prior results in energy management consider the internal optimization processes of PHEVs, this paper focuses on a driver-centric approach that enables the drivers to select the appropriate drive modes for minimizing fuel consumption. Drive modes are driver-selectable pre-set profiles of configurations of powertrain and vehicle parameters. Typical PHEVs have options of drive modes, for example, electric vehicle (EV) mode (that draws fully on battery) and charge sustaining (CS) mode (that utilizes internal combustion engine to charge battery while propelling the vehicle). We develop optimization algorithms that optimize drive mode selection based on trip information, and integrated with path planning to consider intermediate filling and charging stations. We also provide an online algorithm that requires minimal a-priori trip information. We implement our system and evaluate the results empirically on a Chevrolet Volt, which can enable a significant improvement in fuel efficiency.

## CCS Concepts

•**Applied computing** → *Transportation;* •**Theory of computation** → *Dynamic graph algorithms;*

## Keywords

Energy-efficient Transportation, Plug-in Hybrid Electric Vehicles, Fuel Optimization, Path Planning

## 1. INTRODUCTION

Plug-in hybrid electric vehicles (PHEVs) are equipped with rechargeable batteries and electrical machines (which double as electric motors and generators), as well as conventional internal combustion engines (see Fig. 1 (a)). PHEVs are becoming a viable energy-efficient means of transportation, benefited by the convenience of fuel refilling and cheap electrical energy. In addition to using regenerative braking to capture waste energy from braking and engine stop/start assisted by electric motor, PHEVs can also harness the diversity of energy efficiency of electric motors and combustion engines by managing the hybrid energy sources.

Electric motors and combustion engines exhibit different degrees of energy efficiency at various vehicle speeds (see Fig. 1 (b) for an illustration). Electric motors are more effective for energy conversion at a lower speed, while the energy-efficient operating regime of internal combustion engines is around a higher speed. For a very high speed, a combination of electric motor and combustion engine is more efficient. Thus, one can explore the opportunities of charging battery from combustion engine efficiently at a high speed and discharging from battery to propel the vehicle at a low speed (which will be empirically studied in the subsequent section). Given a forecast of vehicle speed profile, it is a crucial research problem to optimize the use of energy sources to reduce the overall energy consumption.

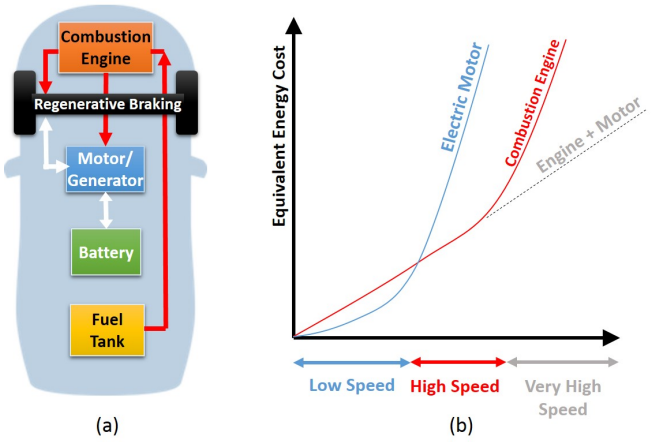


**Figure 1: (a) System components of a plug-in hybrid electric vehicle (PHEV). (b) Comparison of equivalent energy cost of electric motor and combustion engine at different vehicle speeds.**

Many prior results [5,7,13] in energy management consider the internal optimization processes of PHEVs, which assume complete controls of all system components of a PHEV (see Sec. 3). As a departure from prior work, this paper focuses



*e-Energy'16, June 21 - 24, 2016, Waterloo, ON, Canada*



ISBN 978-1-4503-4393-0/16/06…$15.00

DOI: http://dx.doi.org/10.1145/2934328.2934341

on a driver-centric approach that involves drivers' participations and decisions to minimize the fuel consumption. A feasible approach is to optimize the selection of drive modes for a given trip. *Drive modes* are a set of pre-set profiles of configurations of powertrain and other vehicle parameters that are selectable by drivers during driving. For example, Sport mode maximizes the engine performance by allowing larger horsepower, whereas ECO mode suppresses the vehicle performance by constraining acceleration and throttle response. In particular, there are special drive modes for PHEVs that can affect the energy management system.

We describe several generic drive modes for PHEVs:

- *Electric Vehicle* (EV) mode allows the PHEV to draw solely on battery without relying on internal combustion engine.
- *Charge Sustaining* (CS) mode utilizes internal combustion engine to charge battery and propel the PHEV simultaneously.
- *Aggregate Power* (AP) mode combines both electric motor and internal combustion engine to boost the output power.

Although the preceding generic drive modes may not be present in all models of PHEVs, they may be mapped from certain available drive modes (as discussed in Secs. 2, 4.5).

In this paper, we consider general optimization problems of drive mode selection for fuel minimization in two settings:

- *Route-based Optimization*: Given the trip information for a particular route, we find an optimal solution of drive mode selection for each segment of the trip. We also provide an online algorithm that requires minimal a-priori trip information.
- *Integrated Path Planning*: Given the source and destination of a trip, we find an optimal path together with appropriate drive mode selection, taking into account various fuel prices at intermediate filling stations and the availability of battery charging.

In Sec. 4, we formulate the above problems by integer programming problems, which capture several practical aspects of PHEVs (e.g., multi-mode transmission, and vehicle speed dependency in combustion engine management). In Sec. 5, we devise effective algorithms for solving these drive mode selection problems. We also provide fast approximation algorithms for a large problem size.

To demonstrate the practical value of our results, we implement our system and evaluate the results empirically on a Chevrolet Volt in Sec. 8. Validated by real-world data measured in Chevrolet Volt, we observe that our system can enable a significant improvement in fuel efficiency.

We remark that although our current system relies on drivers' inputs of drive modes, the system can be loaded as a software application on the vehicle system platform for automatic drive mode selection, as we expect that the future vehicle platform will support third-party applications.

## 2. BASICS AND BACKGROUND

We first present some basic and background information about PHEVs. The powertrain mechanics of PHEVs can be classified by the following patterns:

- *Series Hybrids*: The internal combustion engine is always connected to the generator to charge battery. The drivetrain is only powered directly by electric motor. Once the state-of-charge of battery becomes low, the internal combustion engine will start to charge battery. Series hybrid vehicles are regarded as range extenders of pure electric vehicles.
- *Parallel Hybrids*: The internal combustion engine and electric motors can operate in tandem to power the drivetrain. A conventional transmission gear train may operate with the internal combustion engine. A power split system is present to combine the parallel power sources. There is a possible clutch to enable the internal combustion engine to charge battery and propel the vehicle simultaneously.
- *Series/Parallel Hybrids*: By using a combination of planetary gear trains, it allows flexible power split between the internal combustion engine and a multiple number of electric motors. An auxiliary electric motor/generator may be present to provide additional performance improvement.

Despite the differences of powertrain mechanics, the internal operations of PHEVs are often transparent to drivers. There are automatic systems to manage the transmission gear, powertrain and hybrid energy sources. Given the steering and petal control status, the automatic system will control the torque, rpm of combustion engine, transmission gears, output power of battery, etc., to match the load of drivetrain [5, 13]. Note that practical control system will normally set the rpm of combustion engine related to the vehicle speed, even for series hybrids in which the combustion engine is not directly connected to the drivetrain. There is a safety hazard for the combustion engine operating in a high speed, when the vehicle is stationary.


(a) (b)

**Figure 2: Options to select drive modes in Chevrolet Volt (model 2013) on (a) the console display unit, or (b) a dedicate button on the center console.**

Although the low-level mechanics are not controllable by drivers, typical vehicles are usually customizable by setting certain high-level drive modes. In following, we describe the available drive modes in several production PHEV models that can affect the behavior of energy management system:

- *Chevrolet Volt* (model 2011-2015) operates as a series hybrid. The available drive modes are Normal, Sport, Mountain and Hold (see Fig. 2). In Normal and Mountain modes, Volt draws only on battery until the state-of-charge drops to 22% and 45% respectively. Then,

Volt turns on internal combustion engine to charge battery, which continues to propel the vehicle. In Hold mode, Volt uses internal combustion engine to maintain the current state-of-charge. Note that Chevrolet Volt (model 2016) operates as a series/parallel hybrid that can utilize internal combustion engine and electric motor in parallel to propel the vehicle.

- *Toyota Prius Plug-in* (model 2012-2015) provides four drive modes: ECO, Normal, Power and EV. Normal mode uses both internal combustion engine and electric motor for propelling the vehicle. It is observed that Prius maintains the state-of-charge to a certain level using internal combustion engine occasionally, as well as from regenerative braking. Power mode increases throttle response of internal combustion engine more than Normal mode. In EV mode, Prius always draws on battery, if there is sufficient state-of-charge, and the vehicle speed is within EV mode range.

- *Ford Fusion Energi* (model 2013-2015) offers three drive modes: EV Now, EV Auto and EV Later. In EV Now mode, Energi draws on battery entirely, if there is sufficient state-of-charge. In EV Auto mode, Energi uses both internal combustion engine and electric motor, depending on the vehicle speed. In EV Later mode, Energi conserves battery for future use, by mostly drawing on internal combustion engine, which possibly charges battery.

Rather than considering model-specific drive modes, we consider four generic drive modes: (1) *Electric Vehicle* (EV) mode that draws solely on battery, (2) *Combustion Engine* (CE) mode that relies solely on internal combustion engine, (3) *Charge Sustaining* (CS) mode that utilizes internal combustion engine to charge battery and propel the vehicle, and (4) *Aggregate Power* (AP) mode that combines both electric motor and internal combustion engine to propel the vehicle.

In Sec. 4, we formulate a general optimization problem of drive mode selection when some of the generic drive modes are considered. We remark that our model is sufficiently general to capture a variety of existing PHEV models. We will discuss the mapping from model-specific drive modes to generic drive modes in Sec. 4.5. In Sec. 8, we particularly validate our model for Chevrolet Volt empirically.

# 3. RELATED WORK

There is a body of work about optimizing energy management systems for PHEVs. For example, [13] uses heuristic control strategy to optimize energy consumption for given torque and speed. A similar concept relying on rule-based management policies has been presented in [5], in which the strategy thresholds are determined using the parameters of efficiency maps of the engines, motors and generators. [4] considers continuous-time optimization control of hybrid energy sources. Some studies focus on sub-optimal solutions that can be computed faster than dynamic programming. Pontryagin's minimum principle is one of sub-optimal approaches using local optimal trajectories [6, 10]. The equivalence consumption minimization strategy provides a sub-optimal solution to a given cost function of variables of PHEV [14]. These prior results often assume complete controls of internal energy management system in PHEVs, and are mostly based on simulations. Our work considers limited control by only selecting the drive modes available in the PHEVs, and evaluate the results on a real-world PHEV.

There are papers about online energy management strategies for PHEVs. For example, [12] considers Lyapunov stochastic optimization for a parallel PHEV. [7] utilizes nonlinear optimization for parallel and serial HEVs. This paper considers competitive online algorithms [2] that can provide proven worst-case guarantees to offline optimal solutions.

Note that most prior papers in PHEV energy management systems ignore several practical issues. For example, practical control system will normally set the rpm of combustion engine related to the vehicle speed, even for series hybrids, because of a safety hazard for the combustion engine operating in a high speed, when the vehicle is stationary. Moreover, production PHEVs often use a variable number of electric motors/generators conditional on the vehicle speed. These practical issues are not considered in most prior papers.

Path planning problems considering various gas prices at intermediate filling stations have been studied in [8]. On the other hand, the problem of optimal routing for charging station and charging time has been studied in [16]. [21] investigates multi-vehicle problem and determines the optimal route with minimum charging time. However, this paper considers a more general path planning problem combined with energy management strategies for PHEVs.

# 4. MODEL AND PROBLEM FORMULATION

Our goal is to develop a systematic study for drive mode selection optimization, based on a generic vehicle model with general vehicle parameters obtainable by measurement or standard vehicle information. We consider a semi-blackbox model of PHEV that is abstracted away from the underlying vehicle control systems. This model will be validated empirically in Sec. 8 with a Chevrolet Volt.

This paper considers a discrete-time setting from time slot $t = 1$ to $t = T$, where the inputs within one time slot are assumed to be sufficiently quasi-static. For brevity, the power and energy within a time slot are referred interchangeably. Let $G_t$ be the fuel tank level and $B_t$ be the state-of-charge of the PHEV at time $t$. $G_0$ and $B_0$ are the initial fuel tank level and state-of-charge respectively.

Define $(v_t, \alpha_t)_{t=1}^{T}$ be the driving profile, where $v_t$ is the vehicle speed and $\alpha_t$ is the gradient of road at time $t$. The driving profile can be obtained by prediction using historic data, or crowd-sourced data collection [17–19, 22]. Note that $v_t, \alpha_t$ are non-negative for all $t$. We assume the energy consumption of PHEV is solely characterized by the driving profile, for example, under moderate weather and traffic conditions.

Let the acceleration be $a_t \triangleq v_t - v_{t\text{-}1}$. The load of drivetrain of a generic vehicle [9, 11, 15] is given by

$$P_t = \frac{\rho_{\mathrm{a}} k_{\mathrm{d}} A_{\mathrm{f}} v_t^3}{2} + \mathsf{m}\mathsf{g}\sin(\alpha_t) v_t + \mathsf{m}\mathsf{g} k_{\mathrm{r}} v_t + \mathsf{m} v_t a_t + \mathsf{c}_0 \quad (1)$$

where $\mathsf{m}$ is the vehicle weight, $\mathsf{g}$ is the gravitational constant, $\rho_{\mathrm{a}}$ is the density of air, $A_{\mathrm{f}}$ is the frontal area of the vehicle, $k_{\mathrm{d}}$ if aerodynamic drag coefficient of the vehicle, $k_{\mathrm{r}}$ is the rolling friction coefficient, and $\mathsf{c}_0$ is the default load (e.g., due to air-conditioning). These parameters can be obtained from standard vehicle information or simple measurement.

Note that $P_t$ can be positive or negative (possibly due to negative $a_t$). Let $P_t^+ = \max\{P_t, 0\}$ and $P_t^- = -\min\{P_t, 0\}$. $P_t^-$ represents the power captured by regenerative breaking.

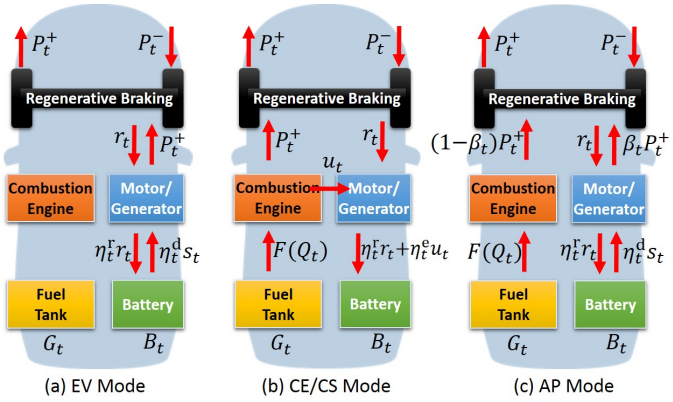


**Figure 3: System models of generic drive modes.**

In the following subsections, we describe the four generic drive modes (EV, CE, CS, AP modes), as illustrated in Fig. 3. These generic drive modes provide abstract representations of the model-specific drive modes in specific PHEV models. We discuss the mapping of model-specific drive modes to generic drive modes in Sec. 4.5. We present an empirical validation study of Chevrolet Volt in Sec. 8.

## 4.1 Electric Vehicle (EV) Mode

In EV mode, the PHEV is only powered by battery, which is also charged by regenerative braking when the vehicle is decelerating or stopping. Let $[\underline{B}, \overline{B}]$ be the allowable range of state-of-charge to operate in EV mode. Let $s_t$ be the power from battery to electric motor (when $P_t^+ \geq 0$), and $r_t$ be the power from generator to battery (when $P_t^- \geq 0$).

If $\underline{B} \leq B_{t\text{-}1} \leq \overline{B}$, then the state-of-charge is given by

$$B_t = B_{t\text{-}1} + \eta_t^{\mathrm{r}} r_t - \eta_t^{\mathrm{d}} s_t \tag{2}$$

subject to $\underline{B} \leq B_t \leq \overline{B}$, $r_t \leq P_t^-$ and $s_t = P_t^+$.

Parameters $\eta_t^{\mathrm{r}} \leq 1$ and $\eta_t^{\mathrm{d}} \geq 1$ denote the charging and discharging efficiency coefficients. Note that $\eta_t^{\mathrm{r}}$ and $\eta_t^{\mathrm{d}}$ may not be constants (which are often assumed to be constants in previous work [5,7,13]). Here, we allow a variable number of generators/motors to be utilized in the PHEV conditional on the driving profile (e.g., observed in production PHEVs like Chevrolet Volt), which induce variable efficiency coefficients.

Note that regenerative braking incurs no fuel cost. Hence, Eqn. (2) and the constraints are equivalent to setting

$$r_t = \min\{P_t^-, \frac{\overline{B} - B_{t\text{-}1}}{\eta_t^{\mathrm{r}}}\} \tag{3}$$

## 4.2 Combustion Engine (CE) Mode

In CE mode, the PHEV is only powered by internal combustion engine. Let the output power from combustion engine at time $t$ be $Q_t$. The fuel tank level is given by

$$G_t = G_{t\text{-}1} - F(Q_t), \text{ where } Q_t = P_t^+ \tag{4}$$

subject to $G_t \geq 0$. $F(\cdot)$ is an increasing convex function that maps the output power to the required amount of fuel.

We also allow the battery to be charged by regenerative braking, if possible. The state-of-charge is given by

$$B_t = B_{t\text{-}1} + \eta_t^{\mathrm{r}} r_t \tag{5}$$

subject to $B_t \leq \overline{B}$ and $r_t \leq P_t^-$. Namely, $r_t = \min\{P_t^-, \frac{\overline{B} - B_{t\text{-}1}}{\eta_t^{\mathrm{r}}}\}$.

## 4.3 Charge Sustaining (CS) Mode

In CS mode, the internal combustion engine is used to propel the vehicle and charge battery simultaneously. Let $u_t$ be the power from engine to charge battery at time $t$. The fuel tank level is given by

$$G_t = G_{t\text{-}1} - F(Q_t), \text{ where } Q_t = P_t^+ + u_t \tag{6}$$

subject to $G_t \geq 0$. The state-of-charge is given by

$$B_t = B_{t\text{-}1} + \eta_t^{\mathrm{r}} r_t + \eta_t^{\mathrm{e}} u_t \tag{7}$$

subject to $B_t \leq \overline{B}$, $r_t \leq P_t^-$, and $u_t \leq C_t$.

$\eta_t^{\mathrm{e}} \leq 1$ denotes the charging efficiency coefficient by combustion engine. Here, we allow possibly different generators used by regenerative braking and combustion engine (e.g., observed in Chevrolet Volt). $C_t$ is the maximum available power to charge battery from combustion engine at time $t$.

Note that practical control systems in PHEVs (e.g., Chevrolet Volt) may set the rpm of combustion engine related to the vehicle speed. Thus, $C_t$ captures the limitation of available power from combustion engine depending on vehicle speed at time $t$.

We assume that the energy management system in PHEV attempts to charge battery up to $C_t$ whenever possible, then Eqns. (6)-(7) and the constraints are equivalent to setting

$$r_t = \min\{P_t^-, \frac{\overline{B} - B_{t\text{-}1}}{\eta_t^{\mathrm{r}}}\}, u_t = \min\{C_t, \frac{\overline{B} - B_{t\text{-}1} - \eta_t^{\mathrm{r}} r_t}{\eta_t^{\mathrm{e}}}\} \tag{8}$$

## 4.4 Aggregate Power (AP) Mode

In AP mode, the PHEV is propelled by internal combustion engine and electric motor (that is powered by battery) together. The state-of-charge is given by

$$B_t = B_{t\text{-}1} + \eta_t^{\mathrm{r}} r_t - \eta_t^{\mathrm{d}} s_t \tag{9}$$

subject to $\underline{B} \leq B_t \leq \overline{B}$, $r_t \leq P_t^-$ and $s_t \leq \beta_t P_t^+$. $\beta_t \leq 1$ is the maximum portion of power contributed by electric motor to drivetrain.

Note that we allow a variable number of generators/motors to be utilized in the PHEV, conditional on the driving profile, which can induce a variable portion of power split by electric motor and combustion engine over time.

The fuel tank level is given by

$$G_t = G_{t\text{-}1} - F(Q_t), \text{ where } Q_t = P_t^+ - s_t \tag{10}$$

subject to $G_t \geq 0$. We assume that the energy management system in PHEV attempts to use electric motor to power the drivetrain by $\beta_t P_t^+$ whenever possible, then Eqns. (9)-(10) and the constraints are equivalent to setting

$$s_t = \min\{\beta_t P_t^+, \frac{B_{t\text{-}1} - \underline{B}}{\eta_t^{\mathrm{d}}}\}, \; r_t = \min\{P_t^-, \frac{\overline{B} - B_{t\text{-}1}}{\eta_t^{\mathrm{r}}}\} \tag{11}$$

**Remark**: Our model is abstracted away from the underlying mechanics, like automatic transmission, powertrain control, etc. But the parameters $\eta_t^{\mathrm{r}}, \eta_t^{\mathrm{d}}, \eta_t^{\mathrm{e}}, C_t, \beta_t$ are sufficiently general to capture the impacts of the underlying mechanics.

## 4.5 Mapping to Generic Drive Modes

We next discuss the mapping of model-specific drive modes to generic drive modes.

- *Chevrolet Volt* has four drive modes: Normal, Sport, Mountain and Hold. We consider the mapping to EV and CS modes. To trigger EV mode, one can enter Normal mode when the state-of-charge is above 22%. To trigger CS mode, one can enter Mountain mode when the state-of-charge is below 45%.
- *Toyota Prius Plug-in* provides four drive modes: ECO, Normal, Power and EV. EV mode is present. Normal mode is a combination of CS and CE modes, whereas Power mode is a combination of AP and CE modes.
- *Ford Fusion Energi* offers three drive modes: EV Now, EV Auto and EV Later. EV mode is present. EV Auto mode is similar to AP mode, whereas EV later mode is similar to CS mode.

The detailed mapping of model-specific drive modes to generic drive modes should be validated by empirical studies. In this paper, we validate on Chevrolet Volt in Sec. 8.

## 4.6 Drive Mode Optimization Problem

Considering the generic drive modes, given a driving profile $(v_t, \alpha_t)_{t=1}^T$, initial state-of-charge $B_0$ and fuel tank level $G_0$, we formulate a fuel minimization problem of PHEV optimizing drive mode optimization as an integer programming problem (DMOP). Let $x_t^{\text{ev}}$, $x_t^{\text{ce}}$, $x_t^{\text{cs}}$, $x_t^{\text{ap}}$ be the binary decision variables if EV, CE, CS, and AP modes are enabled respectively. We define the objective function of DMOP by $\texttt{Cost}(t) \triangleq G_0 - G_t$. Let $x_t = (x_t^{\text{ev}}, x_t^{\text{ce}}, x_t^{\text{cs}}, x_t^{\text{ap}})$.

$$\text{(DMOP)} \qquad \min_{(x_t)_{t=1}^T} \ \texttt{Cost}(T) = G_0 - G_T$$

subject to for all $t \in [1, T]$,

$$G_t = G_{t\text{-}1} - F(Q_t), \tag{12}$$
$$G_t \geq 0, \tag{13}$$
$$Q_t = (1 - x_t^{\text{ev}})P_t^+ + x_t^{\text{cs}} u_t - x_t^{\text{ap}} s_t, \tag{14}$$
$$B_t = B_{t\text{-}1} + \eta_t^{\text{r}} r_t + \eta_t^{\text{e}} u_t - \eta_t^{\text{d}} s_t, \tag{15}$$
$$\underline{B} \leq B_t \leq \overline{B}, \tag{16}$$
$$r_t = \min\{P_t^-, \frac{\overline{B} - B_{t\text{-}1}}{\eta_t^{\text{r}}}\} \tag{17}$$
$$s_t = x_t^{\text{ev}} P_t^+ + x_t^{\text{ap}} \min\{\beta_t P_t^+, \frac{B_{t\text{-}1} - \underline{B}}{\eta_t^{\text{d}}}\} \tag{18}$$
$$u_t = \min\{x_t^{\text{cs}} C_t, \frac{\overline{B} - B_{t\text{-}1} - \eta_t^{\text{r}} r_t}{\eta_t^{\text{e}}}\} \tag{19}$$
$$x_t^{\text{ev}} + x_t^{\text{ce}} + x_t^{\text{cs}} + x_t^{\text{ap}} = 1, \tag{20}$$
$$x_t^{\text{ev}},\ x_t^{\text{ce}},\ x_t^{\text{cs}},\ x_t^{\text{ap}} \in \{0, 1\} \tag{21}$$

**Remark**: DMOP does not always contain a feasible solution, for example, when there is insufficient fuel. If a drive mode is not present, we can disable a certain drive mode in the optimization problem by adding a zero constraint to the respective drive mode. For example, to disable AP mode, we set $x_t^{\text{ap}} = 0$ for all $t$. In particular, we denote by $\text{DMOP}_{\text{cs}}^{\text{ev}}$ that has only EV and CS modes, without CE and AP modes. We apply $\text{DMOP}_{\text{cs}}^{\text{ev}}$ specifically to Chevrolet Volt in Sec. 8.

DMOP is a non-convex problem, even if we relax the integrality constraints (21), because of Cons. (18)-(19). We define a *convexified* problem (cDMOP) with factional solution $x_t$, which is a close approximation to DMOP. By rounding the fractional solutions to integral solutions, this provides a fast approximation solution to solve DMOP.

$$\text{(cDMOP)} \qquad \min_{(x_t, r_t, s_t, u_t)_{t=1}^T} \ \texttt{Cost}(T) = G_0 - G_T$$

subject to for all $t \in [1, T]$,

$$G_t = G_{t\text{-}1} - F(Q_t), \tag{22}$$
$$G_t \geq 0, \tag{23}$$
$$Q_t = (1 - x_t^{\text{ev}})P_t^+ + x_t^{\text{cs}} u_t - x_t^{\text{ap}} s_t, \tag{24}$$
$$B_t = B_{t\text{-}1} + \eta_t^{\text{r}} r_t + \eta_t^{\text{e}} u_t - \eta_t^{\text{d}} s_t, \tag{25}$$
$$\underline{B} \leq B_t \leq \overline{B}, \tag{26}$$
$$r_t \leq P_t^-, \tag{27}$$
$$x_t^{\text{ev}} P_t^+ \leq s_t \leq x_t^{\text{ev}} P_t^+ + x_t^{\text{ap}} \beta_t P_t^+, \tag{28}$$
$$u_t \leq x_t^{\text{cs}} C_t, \tag{29}$$
$$r_t,\ s_t,\ u_t \geq 0 \tag{30}$$
$$x_t^{\text{ev}} + x_t^{\text{ce}} + x_t^{\text{cs}} + x_t^{\text{ap}} = 1, \tag{31}$$
$$0 \leq x_t^{\text{ev}},\ x_t^{\text{ce}},\ x_t^{\text{cs}},\ x_t^{\text{ap}} \leq 1 \tag{32}$$

# 5. OFFLINE SOLUTION

We provide offline solutions of DMOP by dynamic programming. Consider a sub-problem $(\text{DMOP}[B_{t\text{-}1}, B_t, t])$ at time $t$, given the previous state-of-charge $B_{t\text{-}1}$ and current state-of-charge $B_t$:

$$(\text{DMOP}[B_t, B_{t\text{-}1}, t]) \qquad \min_{x_t^{\text{ev}}, x_t^{\text{ce}}, x_t^{\text{cs}}, x_t^{\text{ap}}} \quad F(Q_t)$$
$$\text{subject to Cons. (14)-(21)}$$

Note that when fixing a drive mode $(x_t)$, $\text{DMOP}[B_t, B_{t\text{-}1}, t]$ can be solved in polynomial-time as a linear problem. Let $\texttt{Solve}\big[\text{DMOP}[B_t, B_{t\text{-}1}, t]\big]$ be the minimum-cost solution among the four drive modes. If there is no feasible solution, $\texttt{Solve}\big[\text{DMOP}[B_t, B_{t\text{-}1}, t]\big]$ returns infinite cost.

A dynamic programming approach to solve DMOP is presented in Algorithm DMOP.DP. A similar approach applies to $\text{DMOP}_{\text{cs}}^{\text{ev}}$, when restricting to only CS and EV modes.

**Algorithm 1** $\texttt{DMOP.DP}\big[G_0, B_0\big]$

```
F*_T ← ∞
for each B̂ such that B ≤ B̂ ≤ B̄ do
    (F_T, (x_τ)_{τ=1}^T) ← DP[B̂, T, B_0]
    if F*_T > F_T then
        F*_T ← F_T, (x*_τ)_{τ=1}^T ← (x_τ)_{τ=1}^T
    end if
end for
if F*_T ≤ G_0 then
    return (F*_T, (x*_τ)_{τ=1}^T)
else
    return INFEASIBLE
end if
```

THEOREM 1. *Algorithm* DMOP.DP *gives an optimal solution of* DMOP *in pseudo-polynomial time*[1].

[1]That is, the running time depends polynomially on the unary representation of the input (such as $M$, $N$ and $T$ in the proof of Theorem 1). Note that the running time of a polynomial-time algorithm depends polynomially on the binary representation of the input.

**Algorithm 2** $\texttt{DP}\big[\hat{B}, t, B_0\big]$

**if** $t > 2$ **then**
  $\texttt{cost}_t^{\min} \leftarrow \infty$
  **for each** $B'$ **such that** $\underline{B} \le B' < \hat{B}$ **do**
    $(Q_t, x_t) \leftarrow \texttt{Solve}\big[\text{DMOP}[\hat{B}, B', t]\big]$
    $\big(F_{t-1}, (x_\tau)_{\tau=1}^{t-1}\big) \leftarrow \texttt{DP}\big[B', t-1, B_0\big]$
    **if** $\texttt{cost}_t^{\min} > F(Q_t) + F_{t-1}$ **then**
      $\texttt{cost}_t^{\min} \leftarrow F(Q_t) + F_{t-1}$
      $F_t \leftarrow F(Q_t) + F_{t-1}$
      $x \leftarrow \big((x_\tau)_{\tau=1}^{t-1}, x_t\big)$
    **end if**
  **end for**
  **return** $\big(F_t, (x_\tau)_{\tau=1}^{t}\big)$
**else**
  **return** $\texttt{Solve}\big[\text{DMOP}[\hat{B}, B_0, 1]\big]$
**end if**

Proof. All the steps in DMOP.DP are evidently polynomial except those enumerating over the range of $B_t$. Assume $\underline{B}$, $\overline{B}$, $B_0$, $\beta_t$, $\eta_t^{\mathrm{r}}$, $\eta_t^{\mathrm{d}}$, $\eta_t^{\mathrm{e}}$, $C_t$, $P_t^+$and $P_t^-$ are given as rational number numerator at most $M \in \mathbb{Z}_+$ and common denominator $N \in \mathbb{Z}_+$. Then Eqns. (15)-(19) imply $B_t \in \left\{\frac{M'}{N^2} | M' \in \{0, 1 \ldots, TM^2\}\right\}$, which completes the proof. □

# 6. ONLINE SOLUTION

We present an online algorithm (Online) for DMOP that does not require detailed future driving profile, but only uses general vehicle information and estimate of trip. For simplicity, we consider $\text{DMOP}_{\text{cs}}^{\text{ev}}$ with only EV and CS modes.

Let the inputs be $(\sigma_t)_{t=1}^T = (P_t, \eta_t^{\mathrm{r}}, \eta_t^{\mathrm{d}}, \eta_t^{\mathrm{e}}, C_t, \beta_t)_{t=1}^T$. The problem (DMOP) can be solved optimally, when all inputs $\sigma$ are given in advance. However, $\sigma$ is revealed gradually over time, which requires decisions to be made without future information. An algorithm is called *online*, if the decision at the current time only depends on the instantaneous information before or at the current time slot $t_{\text{now}}$ (i.e., $(\sigma_t)_{t \le t_{\text{now}}}$).

Given input $\sigma$, let $\mathsf{Cost}(\texttt{Alg}[\sigma])$ be the cost of algorithm Alg, and $\mathsf{Opt}(\sigma)$ be the cost of an offline optimal solution (that may rely on an oracle to obtain all future inputs). In competitive analysis for online algorithms [2], *competitive ratio* is a common performance metric, defined as the *worst-case* ratio between the cost of the online algorithm Alg and that of an offline optimal solution, namely,

$$\mathtt{CR}(\texttt{Alg}) \triangleq \max_{\sigma} \frac{\mathsf{Cost}(\texttt{Alg}[\sigma])}{\mathsf{Opt}(\sigma)} \tag{33}$$

To measure the cost-effectiveness in CS mode, define *normalized cost* to be $\frac{F(P_t^+ + u_t)}{P_t^+ + \eta_t^{\mathrm{e}} u_t}$. Algorithm Online is a simple threshold based algorithm that switches to CS mode, if the normalized cost is lower than a threshold $\theta$, or there is insufficient state-of-charge for running EV mode. Otherwise, it will run EV mode, whenever possible. We next determine a proper $\theta$ with a good competitive ratio.

Define the per-unit cost by $f(Q) \triangleq \frac{F(Q)}{Q}$. Note that $F(\cdot)$ is a strictly increasing convex function and $f(Q)$ is an increasing function. Suppose $f_{\min} \le f(Q) \le f_{\max}$ for some constants $f_{\min} \ge f(0)$ and $f_{\max} \le f(\overline{G})$. We assume that $f_{\min}, f_{\max}$ can be estimated in advance for a specific trip. Let $\eta_{\min}^{\mathrm{d}} \triangleq \min_t \eta_t^{\mathrm{d}}$, $\eta_{\min}^{\mathrm{e}} \triangleq \min_t \eta_t^{\mathrm{e}}$, $\eta_{\max}^{\mathrm{e}} \triangleq \max_t \eta_t^{\mathrm{e}}$

**Algorithm 3** $\texttt{Online}\big[\theta, t, (P_t, \eta_t^{\mathrm{r}}, \eta_t^{\mathrm{d}}, \eta_t^{\mathrm{e}}, C_t)\big]$

$x_t^{\mathrm{ev}} \leftarrow 0, x_t^{\mathrm{cs}} \leftarrow 0, u_t \leftarrow 0, s_t \leftarrow 0, r_t \leftarrow 0$
▷ *Charge battery from regenerative braking, if possible*
**if** $P_t^- > 0$ **then**
  $r_t \leftarrow \min\{P_t^-, \frac{\overline{B} - B_{t-1}}{\eta_t^{\mathrm{e}}}\}$
**end if**
$\tilde{u} \leftarrow \min\{C_t, \frac{\overline{B} - B_{t-1} - \eta_t^{\mathrm{r}} r_t}{\eta_t^{\mathrm{e}}}\}$
▷ *Switch to CS mode if below $\theta$ or insufficient SoC*
**if** $\frac{F(P_t^+ + \tilde{u})}{P_t^+ + \eta_t^{\mathrm{e}} \tilde{u}} \le \theta$ **or** $P_t^+ > \frac{B_{t-1} - \underline{B}}{\eta_t^{\mathrm{d}}}$ **then**
  $x_t^{\mathrm{cs}} \leftarrow 1$, $u_t \leftarrow \tilde{u}$
**else**
  $x_t^{\mathrm{ev}} \leftarrow 1$, $s_t \leftarrow P_t^+$
**end if**
**return** $\big(x_t^{\mathrm{ev}}, x_t^{\mathrm{cs}}, r_t, s_t, u_t\big)$

## 6.1 Without Regenerative Braking

For convenience of analysis, we assume the setting without regenerative braking (i.e., $P_t^- = 0$ for all $t$).

Theorem 2. *We consider the initial state-of-charge $B_0 = \underline{B}$ and we require the final state-of-charge to be $B_{T+1} = \overline{B}$. Assuming $P_t^- = 0$ for all $t$, let the threshold in Algorithm* Online *be $\theta = \sqrt{\frac{f_{\max} f_{\min}}{\kappa \eta_{\min}^{\mathrm{d}} \eta_{\max}^{\mathrm{e}}}}$, where $\kappa \triangleq \max\{1, \frac{1}{\eta_{\max}^{\mathrm{e}} \eta_{\min}^{\mathrm{d}}}\}$, then the competitive ratio of* Online *for solving* $\text{DMOP}_{\text{cs}}^{\text{ev}}$ *is*

$$\mathtt{CR}(\texttt{Online}) = \sqrt{\frac{\kappa f_{\max} \eta_{\max}^{\mathrm{e}}}{f_{\min} \eta_{\min}^{\mathrm{d}}}} \frac{1}{\eta_{\min}^{\mathrm{e}}} \tag{34}$$

Proof. Since the initial state-of-charge $B_0 = \underline{B}$, $P_t^+$ at any time $t$ must be satisfied by running CS mode before or at $t$. Also, since we require the final state-of-charge to be $B_{T+1} = \overline{B}$, always charging the battery up to $\overline{B}$ will not incur unnecessary charging at the final time $T$.

For each $P_t^+$, let $\mathsf{Cost}[\texttt{Online}, P_t^+]$ and $\mathsf{Cost}[\texttt{Opt}, P_t^+]$ be the incurred cost by Online and offline optimal solution Opt, respectively. Each $P_t^+$ can be satisfied by two cases in Online:

(C1) *Running CS mode at time $t$*: There are two sub-cases:

(C1.1) The battery has not been charged sufficiently by combustion engine in CS mode before $t$ by Online. The incurred cost for $P_t^+$ of Online at time $t$ is at most $f_{\max} P_t^+$. But Opt may charge the battery sufficiently by combustion engine in CS mode before $t$ with a cost at least $\theta \eta_t^{\mathrm{d}} \eta_{\min}^{\mathrm{e}} P_t^+$. Otherwise, Online would also charge the battery sufficiently before $t$. The ratio between cost of Online over Opt is upper bounded by

$$\frac{\mathsf{Cost}[\texttt{Online}, P_t^+]}{\mathsf{Cost}[\texttt{Opt}, P_t^+]} \le \frac{f_{\max}}{\theta \eta_{\min}^{\mathrm{d}} \eta_{\min}^{\mathrm{e}}} \tag{35}$$

(C1.2) The normalized cost is below $\theta$ at $t$, which incurs a cost for $P_t^+$ at most $\theta P_t^+$. But Opt incurs a cost at least $f_{\min} \eta_t^{\mathrm{d}} \eta_{\min}^{\mathrm{e}} P_t^+$. The ratio between cost of Online over Opt is upper bounded by

$$\frac{\mathsf{Cost}[\texttt{Online}, P_t^+]}{\mathsf{Cost}[\texttt{Opt}, P_t^+]} \le \frac{\theta}{f_{\min} \eta_{\min}^{\mathrm{d}} \eta_{\min}^{\mathrm{e}}} \tag{36}$$

(C2) *Running EV mode at time t*: The battery has been charged by combustion engine in CS mode at some time slot before $t$ by `Online`, which incurs a cost for $P_t^+$ at most $\theta\eta_t^{\mathrm{d}}\eta_{\max}^{\mathrm{e}}P_t^+$. But `Opt` incurs a cost at least $f_{\min}\eta_t^{\mathrm{d}}\eta_{\min}^{\mathrm{e}}P_t^+$. The ratio between cost of `Online` over `Opt` is upper bounded by

$$\frac{\mathsf{Cost}[\texttt{Online}, P_t^+]}{\mathsf{Cost}[\texttt{Opt}, P_t^+]} \leq \frac{\theta\eta_{\max}^{\mathrm{e}}}{f_{\min}\eta_{\min}^{\mathrm{e}}} \tag{37}$$

Let $\kappa \triangleq \max\{1, \frac{1}{\eta_{\max}^{\mathrm{e}}\eta_{\min}^{\mathrm{d}}}\}$. Therefore, the competitive ratio of `Online` is upper bounded by

$$\mathtt{CR}(\texttt{Online}) = \max_{\sigma} \frac{\sum_{t=1}^{T}\mathsf{Cost}[\texttt{Online}, P_t^+]}{\sum_{t=1}^{T}\mathsf{Cost}[\texttt{Opt}, P_t^+]} \tag{38}$$

$$\leq \max_{\sigma,t} \frac{\mathsf{Cost}[\texttt{Online}, P_t^+]}{\mathsf{Cost}[\texttt{Opt}, P_t^+]} \leq \max\left\{\frac{f_{\max}}{\theta\eta_{\min}^{\mathrm{d}}\eta_{\min}^{\mathrm{e}}}, \frac{\theta\kappa\eta_{\max}^{\mathrm{e}}}{f_{\min}\eta_{\min}^{\mathrm{e}}}\right\}$$

An adversary will select the worst among the two cases. In order to minimize the competitive ratio, we set

$$\frac{f_{\max}}{\theta\eta_{\min}^{\mathrm{d}}\eta_{\min}^{\mathrm{e}}} = \frac{\theta\kappa\eta_{\max}^{\mathrm{e}}}{f_{\min}\eta_{\min}^{\mathrm{e}}} \quad \Rightarrow \quad \theta = \sqrt{\frac{f_{\max}f_{\min}}{\kappa\eta_{\min}^{\mathrm{d}}\eta_{\max}^{\mathrm{e}}}} \tag{39}$$

Thus, we obtain the competitive ratio as

$$\mathtt{CR}(\texttt{Online}) = \sqrt{\frac{\kappa f_{\max}\eta_{\max}^{\mathrm{e}}}{f_{\min}\eta_{\min}^{\mathrm{d}}}}\frac{1}{\eta_{\min}^{\mathrm{e}}} \tag{40}$$

□

**Remark**: If $f_{\min}, f_{\max}$ are not known in advance, Algorithm `Online` can be adapted to estimate these parameters dynamically. First, set $f_{\min} = f_{\max} = f(Q_1)$. Then $f_{\min}, f_{\max}$ are updated to be the maximum and minimum $f(Q_t)$ observed so far at time slot $t$. If $T$ is relatively large, the estimated $f_{\min}, f_{\max}$ will converge to the true values.

# 7. PATH PLANNING WITH DRIVE MODE OPTIMIZATION

We consider an integrated optimization problem that incorporates both path planning and drive mode optimization for a PHEV, with the following features:

- Multiple paths between the source and destination.
- Possible intermediate nodes in each path to provide fuel refilling or battery charging.

We first define several notations as follows. A road network is represented by a connected directed graph $\mathcal{G} = (\mathcal{N}, \mathcal{E})$ that connects from the source $\mathsf{v_s}$ to the destination $\mathsf{v_d}$. For each edge $e = (\mathsf{u}, \mathsf{v}) \in \mathcal{E}$, $\mathsf{u}$ may be a stop, such that the PHEV can receive refilling of fuel at price $g_{\mathsf{u}}$ per unit, or battery charging at most $E_{\mathsf{u}}$ unit at price $h_{\mathsf{u}}$ per unit. Let $\mathcal{P}$ be the set of paths connecting $\mathsf{v_s}$ and $\mathsf{v_d}$. We label the edges in each $P \in \mathcal{P}$ by $(e_1, e_2, ..., e_{n(P)})$ and write $e_i = (\mathsf{u}_i, \mathsf{v}_i)$. Let $T(e)$ be the number of time slots required for traveling $e$. Let $G_{e,t}$ be the initial fuel tank level at time $t$ traveling $e$. Let the fuel tank capacity be $\overline{G}$. Let the initial fuel level and state-of-charge be $G_{e_0,T(e_0)} = G_0$ and $B_{e_0,T(e_0)} = B_0$.

The path planning problem with drive mode optimization (PPDM) is formulated as follows.

$$\text{(PPDM)} \min_{(x_{e,t})_{t=1,e\in P}^{T(e)}, P\in\mathcal{P}} \sum_{i=1}^{n(P)} g_{\mathsf{u}_i}(G_{e_i,0} - G_{e_{i\text{-}1},T(e_{i\text{-}1})}) + h_{\mathsf{u}_i}(B_{e_i,0} - B_{e_{i\text{-}1},T(e_{i\text{-}1})})$$

subject to for all $i \in [1, n(P)], t \in [1, T(e_i)]$

$$G_{e_i,0} \leq \overline{G}, \tag{41}$$
$$G_{e_i,t} = G_{e_i,t\text{-}1} - F(Q_{e_i,t}), \tag{42}$$
$$G_{e_i,t} \geq 0, \tag{43}$$
$$Q_{e_i,t} = (1 - x_{e_i,t}^{\mathrm{ev}})P_{e_i,t}^+ + x_{e_i,t}^{\mathrm{cs}}u_{e_i,t} - x_{e_i,t}^{\mathrm{ap}}s_{e_i,t}, \tag{44}$$
$$B_{e_i,t} = B_{e_i,t\text{-}1} + \eta_{e_i,t}^{\mathrm{r}}r_{e_i,t} + \eta_{e_i,t}^{\mathrm{e}}u_{e_i,t} - \eta_{e_i,t}^{\mathrm{d}}s_{e_i,t}, \tag{45}$$
$$B_{e_{i\text{-}1},T(e_{i\text{-}1})} - B_{e_i,0} \leq E_{\mathsf{u}_i} \tag{46}$$
$$r_{e_i,t} = \min\{P_{e_i,t}^-, \frac{\overline{B} - B_{e_i,t\text{-}1}}{\eta_{e_i,t}^{\mathrm{r}}}\} \tag{47}$$
$$s_{e_i,t} = x_{e_i,t}^{\mathrm{ev}}P_{e_i,t}^+ + x_{e_i,t}^{\mathrm{ap}}\min\{\beta_{e_i,t}P_{e_i,t}^+, \frac{B_{e_i,t\text{-}1} - \underline{B}}{\eta_{e_i,t}^{\mathrm{d}}}\} \tag{48}$$
$$u_{e_i,t} = \min\{x_{e_i,t}^{\mathrm{cs}}C_{e_i,t}, \frac{\overline{B} - B_{e_i,t\text{-}1} - \eta_{e_i,t}^{\mathrm{r}}r_{e_i,t}}{\eta_{e_i,t}^{\mathrm{e}}}\} \tag{49}$$
$$x_{e_i,t}^{\mathrm{ev}} + x_{e_i,t}^{\mathrm{ce}} + x_{e_i,t}^{\mathrm{cs}} + x_{e_i,t}^{\mathrm{ap}} = 1, \tag{50}$$
$$x_{e_i,t}^{\mathrm{ev}},\ x_{e_i,t}^{\mathrm{ce}},\ x_{e_i,t}^{\mathrm{cs}},\ x_{e_i,t}^{\mathrm{ap}} \in \{0,1\} \tag{51}$$

## 7.1 Dynamic Programming

We next employ dynamic programming to solve PPDM.

### 7.1.1 Uniform Cost Case

We first consider the *uniform* case with identical fuel price ($g_{\mathsf{u}} = 1$ and $h_{\mathsf{u}} = 0$ for all $\mathsf{u}$). Consider a path $P = (e_1, \ldots, e_{n(P)}) \in \mathcal{P}$. By Eqn. (42), we obtain

$$G_{e_i,0} - G_{e_i,T(e_i)} = \sum_{t=1}^{T(e_i)} F(Q_{e_i},t), \text{ for } i = 2, \ldots, n(P) \tag{52}$$

By Eqn. (41) and Eqn. (43), we obtain

$$\sum_{t=1}^{T(e_i)} F(Q_{e_i},t) \leq \overline{G} \tag{53}$$

Thus, we can rewrite PPDM as follows:

$$\text{(uPPDM)} \min_{(x_{e,t})_{t=1,e\in P}^{T(e)}, P\in\mathcal{P}} \sum_{i=1}^{n(P)}\sum_{t=1}^{T(e_i)} F(Q_{e_i,t})$$

subject to Eqns. (53) and (44)-(51)

To solve uPPDM, we construct a weighted directed graph $\widetilde{\mathcal{G}} = (\widetilde{\mathcal{N}}, \widetilde{\mathcal{E}}, w)$ as follows. Let $\mathcal{F}_e(B, B')$ be the optimal solution of DMOP for edge $e \in \mathcal{E}$, when the $B_{e,0} = B$ and $B_{e,T(e)} = B'$. For each edge $e \in E$, this value can be obtained by dynamic programming as explained in Section 5. For every node $\mathsf{v} \in \mathcal{N}$ and every $B$ in the range $[\underline{B}, \overline{B}]$, we create a node $\mathsf{v}_B \in \mathcal{N}'$. If $e = (\mathsf{u}, \mathsf{v}) \in \mathcal{E}$ then we have an edge $(\mathsf{u}_B, \mathsf{v}_{B''}) \in \widetilde{\mathcal{E}}$ with weight $w(\mathsf{u}_B, \mathsf{v}_{B''}) = \mathcal{F}_e(B, B')$, for every[2] $B, B', B''$ in the range $[\underline{B}, \overline{B}]$ such that $\mathcal{F}_e(B, B') \leq \overline{G}$ and $B' \leq B'' \leq B' + E_{\mathsf{u}}$. In addition, we create a source

[2]Note that, since battery charging at each node is for free, it is enough to construct only one edge corresponding to

$$C[\mathsf{u}_B,1,g]=\begin{cases}\min\limits_{B\le B'\le\min\{B+E_{\mathsf{u}},\overline{B}\}}\Big((w(\mathsf{u}_{B'},\mathsf{t})-g)g_{\mathsf{u}}+h_{\mathsf{u}}(B'-B)\Big), & \text{if } g\le w(\mathsf{u}_{B'},\mathsf{t})\le\overline{G}\\ \infty, & \text{otherwise}\end{cases}\tag{54}$$

$$C[\mathsf{u}_B,q,g]=\min_{\substack{B\le B'\le\min\{B+E_{\mathsf{u}},\overline{B}\},\mathsf{v}_{B''}:\\ w(\mathsf{u}_{B'},\mathsf{v}_{B''})\le\overline{G}}}\begin{cases}C[\mathsf{v}_{B''},q\text{-}1,0]+(w(\mathsf{u}_{B'},\mathsf{v}_{B''})-g)g_{\mathsf{u}}+h_{\mathsf{u}}(B'\text{-}B), & \text{if } g_{\mathsf{v}}\le g_{\mathsf{u}} \text{ and } g\le w(\mathsf{u}_{B'},\mathsf{v}_{B''})\\ C\Big[\mathsf{v}_{B''},q\text{-}1,\overline{G}\text{-}w(\mathsf{u}_{B'},\mathsf{v}_{B''})\Big]+(\overline{G}\text{-}g)g_{\mathsf{u}}+h_{\mathsf{u}}(B'\text{-}B), & \text{if } g_{\mathsf{v}}>g_{\mathsf{u}}\end{cases}\tag{55}$$

node $\mathsf{s}\in\widetilde{\mathcal{N}}$ with edges $(\mathsf{s},(\mathsf{v}_{\mathsf{s}})_{B''})$, for each $B''$ in the range $[B_0,\min\{B_0+E_{\mathsf{v}_{\mathsf{s}}},\overline{B}\}]$, having weight $\overline{G}-G_0$ and cost $g_{\mathsf{s}}=0$; and a destination node $\mathsf{t}\in\widetilde{\mathcal{N}}$ with edges $((\mathsf{v}_{\mathsf{d}})_B,\mathsf{t})$ having weight 0, for all $B$ in the range $[\underline{B},\overline{B}]$.

Then the optimal solution to uPPDM can be obtained by finding an $(\mathsf{s},\mathsf{t})$-shortest path in the graph $\widetilde{\mathcal{G}}$, with the (non-negative) weights $w(\cdot,\cdot)$ interpreted as distances.

### 7.1.2 General Case

Next, we consider the more general case when the fuel cost per unit $g_{\mathsf{u}}$ may not be equal at all nodes $\mathsf{u}\in\mathcal{N}$, and with the additional restriction that the PHEV can make at most $\Delta$ stops between $\mathsf{v}_{\mathsf{s}}$ and $\mathsf{v}_{\mathsf{d}}$. We assume that battery charging (at the stop) is allowed only when the vehicle stops for fuel refill[3]. Additionally, we assume that battery charging at node $\mathsf{u}$ costs $h_{\mathsf{u}}$ per unit, and the objective is to minimize the combined fuel cost and battery charging cost. The basic idea is to adopt the dynamic program for the so-called *Gas Station Problem* in [8], and apply it to the graph $\widetilde{\mathcal{G}}$ constructed above. We define the graph $\mathcal{G}_0$ as the subgraph of $\widetilde{\mathcal{G}}$ such that $E_e=0$ for all $e$.

Following [8], for any node $\mathsf{v}_B\in\widetilde{\mathcal{N}}$ we define:

$$\mathscr{G}(\mathsf{v}_B)\triangleq\Big\{\overline{G}-w(\mathsf{u}^B,\mathsf{v}_{B'})\mid\mathsf{v}_{\mathsf{B}'}\in\widetilde{\mathcal{N}},\ g_{\mathsf{u}}<g_{\mathsf{v}}\ \text{and } w(\mathsf{u}_B,\mathsf{v}_{B'})<\overline{G}\Big\}\cup\{0\};\tag{56}$$

Namely, $\mathscr{G}(\mathsf{v}_B)$ are the set of fuel levels that are sufficient to consider at node $\mathsf{v}_B$.

Let $C[\mathsf{u}_B,q,g]$ be the minimum cost of going (in the graph $\widetilde{\mathcal{G}}$) from $\mathsf{u}_B$ to $\mathsf{t}$ using $q$ stops (including $\mathsf{u}_B$), when the fuel level at $\mathsf{u}_B$ is $g$. Then we can write the recurrence equations (54)-(55) for $C[\mathsf{u}_B,q,g]$ for any $g\in\mathscr{G}(\mathsf{v}_B)$ and $2\le q\le\Delta$. $w(\mathsf{u}_{B'},\mathsf{v}_{B''})$ is the shortest distance (with respect to $d$) between (not necessarily adjacent nodes) $\mathsf{u}_{B'}$ and $\mathsf{v}_{B''}$ in the graph $\mathcal{G}_0$ (note that we use $\mathcal{G}_0$ as the PHEV does not make any stop between $\mathsf{u}_{B'}$ and $\mathsf{v}_{B''}$). The algorithm is described in PPDM.DP.

THEOREM 3. *Algorithm* PPDM.DP *computes an optimal solution for* PPDM *in pseudo-polynomial time.*

PROOF. All the steps in PPDM.DP are evidently polynomial except that the dynamic program has to enumerate over the range of $B_t$. By the same argument in the proof of Theorem 1, this range is polynomial in the unary size of the input, and hence PPDM.DP is pseudo-polynomial.

To see that PPDM.DP is correct, we use Lemma 2.1 in [8] which states that in an optimal path, if $\mathsf{u}_{B'}$ and $\mathsf{v}_{B''}$ are two consecutive nodes at which the vehicle stops for a fuel-refill, then the fuel level upon reaching $\mathsf{v}_{B''}$ must be either 0, if $g_{\mathsf{v}}\le g_{\mathsf{u}}$, or $\overline{G}-w(\mathsf{u}_{B'},\mathsf{v}_{B''})$, if $g_{\mathsf{v}}>g_{\mathsf{u}}$. (Otherwise, the overall fuel cost can be reduced by an exchange argument.)

To see Eqn. (54), note that if the vehicle has to reach $\mathsf{t}$ form $\mathsf{u}$ in one hop, when the fuel level at $\mathsf{u}$ is $g$ and the state-of-charge is $B$, then it has the option of recharging the battery up to $B'\in[B,\min\{B+E_{\mathsf{u}},\overline{B}\}]$, for a cost of $h_{\mathsf{u}}(B'-B)$ and refill the tank just enough to reach $\mathsf{t}$, for a cost of $(w(\mathsf{u}_{B'},\mathsf{t})-g)g_{\mathsf{u}}$. Note that we use $w(\mathsf{u}_{B'},\mathsf{t})$ which is the distance between $\mathsf{u}_{B'}$ and $\mathsf{t}$ in $\mathcal{G}_0$, and hence without any further recharging; also $w(\mathsf{u}_{B'},\mathsf{t})\le\overline{G}$ must hold, otherwise, it is impossible to drive from $\mathsf{u}_{\mathsf{B}'}$ to $\mathsf{t}$ without refilling.

To see Eqn. (55), note that if the vehicle has to reach $\mathsf{t}$ form $\mathsf{u}$ in $q$ hops, when the fuel level at $\mathsf{u}$ is $g$ and the state-of-charge is $B$, then according to the above mentioned lemma, it has the following options: (1) recharge the battery up to $B'\in[B,\min\{B+E_{\mathsf{u}},\overline{B}\}]$, for a cost of $h_{\mathsf{u}}(B'-B)$, and refill the tank just enough to reach the next stop $\mathsf{v}$ at a state-of-charge $B''$, for a fuel cost of $(w(\mathsf{u}_{B'},\mathsf{v}_{\mathsf{B}''})-g)g_{\mathsf{u}}$; in this case we must have $g_{\mathsf{v}}\le g_{\mathsf{u}}$, or (2) recharge the battery upto $B'\in[B,\min\{B+E_{\mathsf{u}},\overline{B}\}]$, for a cost of $h_{\mathsf{u}}(B'-B)$, and fill up the tank, then reach the next stop $\mathsf{v}$, at state-of-charge $B''$ and fuel level $\overline{G}-w(\mathsf{u}_{B'},\mathsf{v}_{B''})$, for a fuel cost of $(\overline{G}-g)g_{\mathsf{u}}$; in this case we must have $g_{\mathsf{v}}>g_{\mathsf{u}}$. In both cases, the vehicle has to go from $\mathsf{v}_{B''}$ to $\mathsf{t}$ in $q-1$ hops. □

**Remark**: One can obtain an approximation solution for PPDM by considering cDMOP with flow constraints. We skip the details due to the paucity of space.

# 8. EVALUATION

We implement our system (as a smartphone app) and evaluate it empirically on a Chevrolet Volt (Model 2013). Validated by real-world data measured on Volt, we observe our system enables a significant improvement in fuel efficiency.

## 8.1 Vehicle Model Validation

We first estimate the efficiency coefficients $\eta_t^{\mathrm{r}},\eta_t^{\mathrm{d}},\eta_t^{\mathrm{e}}$. Our approach utilizes the On-board Diagnostics (OBD) dongle [20] to query the relevant data from Chevrolet Volt (e.g., battery voltage, battery current, motor voltage, motor current, fuel rate and vehicle speed). We then use regression models to compute $\eta_t^{\mathrm{r}},\eta_t^{\mathrm{d}},\eta_t^{\mathrm{e}}$ according to driving profile. Our testing environment is mostly flat, and hence, we set gradient of road $\alpha_t=0$.

Let the measured power of battery be $P_t^{\mathsf{B}}$, which is related to the load of drivetrain as follows:

$$P_t^{\mathsf{B}+}=P_t^{+}\eta_t^{\mathrm{d}},\quad P_t^{\mathsf{B}-}=P_t^{-}\eta_t^{\mathrm{r}}\tag{57}$$

$B''=\min\{B'+E_{\mathsf{u}},\overline{B}\}$; however, defining the graph in this general form allows to extend the dynamic program for the case when there is a cost for charging each unit of battery at node $\mathsf{u}$.

[3]This assumption can be removed if we assume battery charging cost is 0 at all nodes.

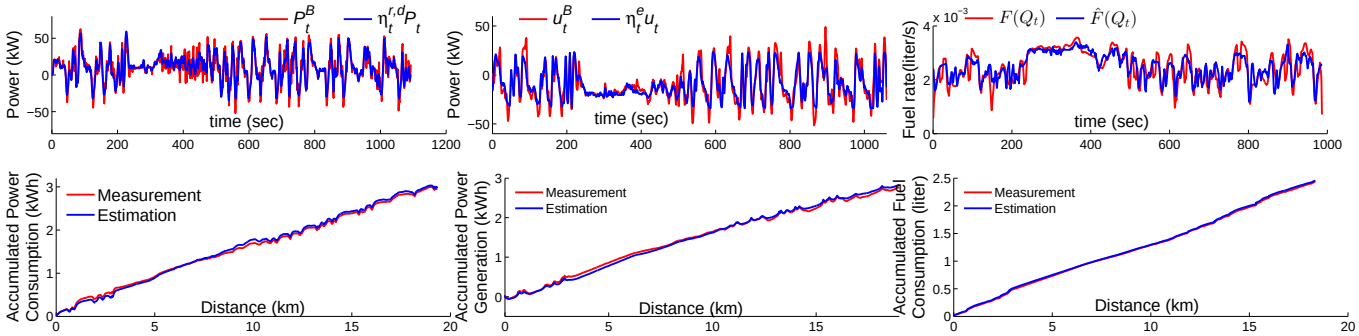


(a) Estimation of $\eta_t^{\mathrm{r}}, \eta_t^{\mathrm{d}}$. (b) Estimation of $\eta_t^{\mathrm{e}}$. (c) Estimation of $F(\cdot)$.

**Figure 4: Estimation of efficiency coefficients and comparisons to the measurements.**

**Algorithm 4** PPDM.DP$\left[G_0, B_0\right]$

Construct graph $\widetilde{\mathcal{G}} = (\widetilde{\mathcal{N}}, \widetilde{\mathcal{E}}, d)$ and extract subgraph $\mathcal{G}_0$
Find all-pairs shortest-distances $\{w(u_B, v_{B'})\}_{u_B, v_{B'}}$ in $\mathcal{G}_0$
Let $\mathcal{B}$ be the discretized range between $\underline{B}$ and $\overline{B}$
for each $B \in \mathcal{B}$, $\mathtt{v} \in \mathcal{N}$ do
  Let $\mathscr{G}(\mathtt{v}_B)$ be as given by Eqn. (56)
end for
for each $B \in \mathcal{B}$, $\mathtt{u} \in \mathcal{N}$, $q \in \{1, ..., \Delta\}$ and $g \in \mathscr{G}(\mathtt{u}_B)$ do
  $C[u_B, q, g] \leftarrow \infty$
end for
▷ *Compute the base case (Eqn. (54))*
for each $B \in \mathcal{B}$, $\mathtt{u} \in \mathcal{N}$, and $g \in \mathscr{G}(\mathtt{u}_B)$ do
  for $B' \in \mathcal{B}$ such that $\underline{B} \le B' \le \min\{B + E_{\mathtt{u}}, \overline{B}\}$ do
    if $g \le w(\mathtt{u}_{B'}, \mathtt{t}) \le \overline{G}$ and $(w(\mathtt{u}_{B'}, \mathtt{t}) - g)g_{\mathtt{u}} + h_{\mathtt{u}}(B' - B) < C[u_B, 1, g]$ then
      $C[u_B, 1, g] \leftarrow (w(\mathtt{u}_{B'}, \mathtt{t}) - g)g_{\mathtt{u}} + h_{\mathtt{u}}(B' - B)$
    end if
  end for
end for
▷ *Compute the general case (Eqn. (55))*
for each $B \in \mathcal{B}$, $\mathtt{u} \in \mathcal{N}$, $q \in \{1, \ldots, \Delta\}$, and $g \in \mathscr{G}(\mathtt{u}_B)$ do
  for $B' \in \mathcal{B}$ such that $\underline{B} \le B' \le \min\{B + E_{\mathtt{u}}, \overline{B}\}$ do
    for $B'' \in \mathcal{B}$ and $\mathtt{v} \in \mathcal{N}$ such that $w(\mathtt{u}_{B'}, \mathtt{v}_{B''}) \le \overline{G}$ do
      if $g_{\mathtt{v}} \le g_{\mathtt{u}}$, $g \le w(\mathtt{u}_{B'}, v_{B''})$ and $C[\mathtt{v}_{B''}, q\text{-}1, 0] + (w(\mathtt{u}_{B'}, \mathtt{v}_{B''})\text{-}g)g_{\mathtt{u}} + h_{\mathtt{u}}(B'\text{-}B) < C[u_B, q, g]$ then
        $C[u_B, q, g] \leftarrow C[\mathtt{v}_{B''}, q\text{-}1, 0] + (w(\mathtt{u}_{B'}, \mathtt{v}_{B''})\text{-}g)g_{\mathtt{u}} + h_{\mathtt{u}}(B'\text{-}B)$
      else
        if $g_{\mathtt{v}} > g_{\mathtt{u}}$ and $C\left[\mathtt{v}_{B''}, q\text{-}1, \overline{G}\text{-}w(\mathtt{u}_{B'}, \mathtt{v}_{B''})\right] + (\overline{G}\text{-}g)g_{\mathtt{u}} + h_{\mathtt{u}}(B'\text{-}B) < C[u_B, q, g]$ then
          $C[u_B, q, g] \leftarrow C\left[\mathtt{v}_{B''}, q\text{-}1, \overline{G}\text{-}w(\mathtt{u}_{B'}, \mathtt{v}_{B''})\right] + (\overline{G}\text{-}g)g_{\mathtt{u}} + h_{\mathtt{u}}(B'\text{-}B)$
        end if
      end if
    end for
  end for
end for
return $\min_{1 \le q \le \Delta} C[\mathtt{s}, q, 0]$

We estimate $\eta_t^{\mathrm{r}}, \eta_t^{\mathrm{d}}$ by the following regression model:

$$\eta_t^{r,d} = \lambda_1 v_t^2 + \lambda_2 v_t + \lambda_3 a_2^{+2} + \lambda_4 a_t^{+} + \lambda_5 a_t^{-2} + \lambda_6 a_t^{-} + \lambda_7 \quad (58)$$

where $a_t^+ \triangleq \max\{v_t - v_{t-1}, 0\}$ and $a_t^- \triangleq \max\{v_{t-1} - v_t, 0\}$. Note that if $a_t^+ > 0$, then $a_t^- = 0$.

Let the measured power from combustion engine to charge the battery be $u_t^{\mathrm{B}} = \eta_t^e u_t$, where $\eta_t^{\mathrm{e}}$ is estimated by:

$$\eta_t^e = \mu_1 v_t^2 + \mu v_t + \mu_3 a_2^{+2} + \mu_4 a_t^{+} + \mu_5 a_t^{-2} + \mu_6 a_t^{-} + \mu_7 \quad (59)$$

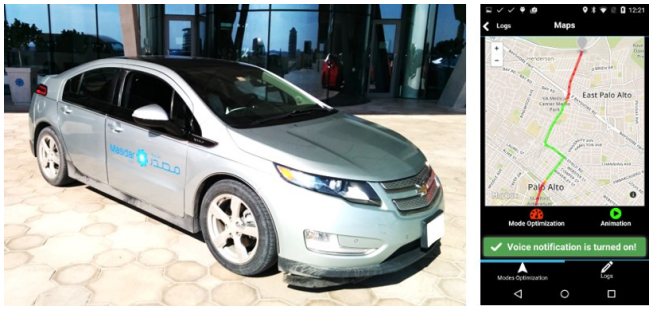

**Figure 5: A Chevrolet Volt for experiment and smartphone app implementation.**

We also estimate fuel consumption function $F(\cdot)$ by:

$$\hat{F}(Q_t) = \gamma_1 Q_t^2 + \gamma_2 Q_t + \gamma_3 \quad (60)$$

Once the parameters of regression models are determined using the collected data from OBD, we compare the estimated accumulative power consumption, generation, and fuel consumption (integrated over time) and the actual measurements in Fig.4. We observe good accuracy of our model. We also observe that $C_t$ is linearly proportional to $P_t^+$.

## 8.2 Drive Mode Optimization

After obtaining the estimated parameters for the vehicle model from experiments, we apply our drive mode selection algorithms to Chevrolet Volt. We only consider $\mathrm{DMOP}_{\mathrm{cs}}^{\mathrm{ev}}$ with two drive modes: EV mode and CS mode.

We compare the optimal solutions by dynamic programming, approximation solutions and online solutions. We consider two driving profiles for case studies:

1. FTP-75 (Federal Test Procedure [1]) has been used for light-duty vehicles in emission certification and fuel economy testing in the US. 20 cycles of FTP-75 are repeated to form a longer driving profile.

2. We collected driving profile from Chevrolet Volt for a driver commuting between home and office.

The initial state-of-charge and route information is summarized in Table 1. Note that though the battery capacity is 16.5 kWh, Chevrolet Volt will use battery from state-of-charge 85% to 22%, which means that the maximum usable battery capacity is 10.4 kWh when it is fully charged. In

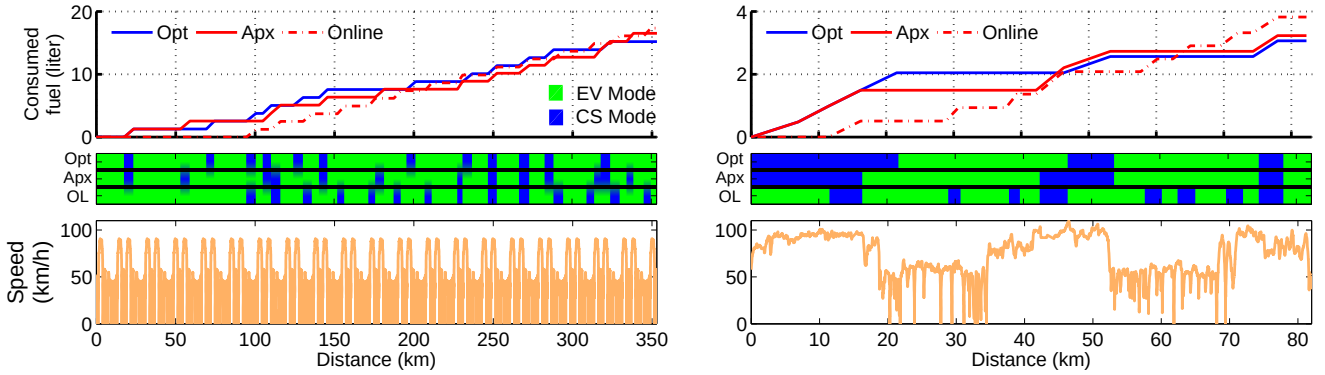


(a) Trip I (b) Trip II

**Figure 6: Fuel consumption and the driving mode selection outcomes of different methods for a single trip.**

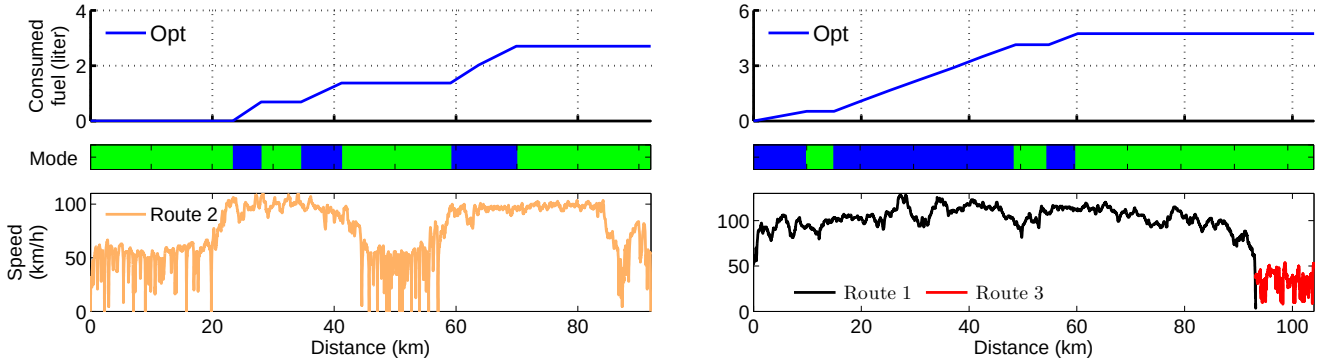


(b) Case I (d) Case II

**Figure 7: Fuel consumption and the driving mode selection outcomes of different methods for path planning.**

these driving profiles, the amount of energy captured by regenerative braking is small.

| Trip | Length(km) | Average Speed(km/h) | Initial SoC(kWh) |
|---|---|---|---|
| I | 353 | 34.1 | 10 |
| II | 82 | 57.2 | 2 |

**Table 1: Simulation setting for mode optimization**

Figs.6(a)-6(b) depict the solutions of driving mode selection for Trips I and II with different methods: `Opt` using dynamic programming, `Apx` using approximation solutions, and `Online`. We observe that `Apx` has a very similar fuel consumption with `Opt`, whereas `Online` has slightly more fuel consumption than `Opt`. We also show the driving mode selection outcomes by each method in the blue-green colored charts below the fuel consumption plots. We observe that the outcomes of `Apx` resemble those of `Opt`, whereas `Online` tends to run CS modes less often.

## 8.3 Integrated Path Planning

In this section, we evaluate our solutions on path planning with drive mode selection for Chevrolet Volt. We only consider $\text{PPDM}_{\text{cs}}^{\text{ev}}$ with two drive modes: EV mode and CS mode. We conduct a case study on a real-world road network with collected driving profiles on each route. Fig.8 depicts the road network with four major stops, with the respective average speed and length of each route. Route(1) is a highway, whereas other routes are regional roads. Node A is the source, whereas node B is the destination. We consider two particular cases with different initial state-of-charge, as summarized in Table 2.

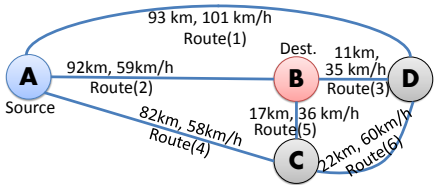


**Figure 8: Road network for case study of path planning.**

| Case | Initial SoC(kWh) | Optimal Path | Consumed Fuel(liter) |
|---|---|---|---|
| I | 5 | 2 | 3.16 |
| II | 2 | 1→3 | 4.73 |

**Table 2: Two cases with different initial state-of-charge.**

In this case study, we observe that different optimal path

will be selected as a result of different initial state-of-charge. For Case I, the battery is initially half-full. Hence, route(2) is the most energy-efficient, because there are more stop-and-go events for EV mode. The result is depicted in Fig. 7(a). On the other hand, Case II selects a different path, the battery is initially low. Hence, it is most energy-efficient to take the highway (i.e., route(1)) which can use CS mode to charge battery for running EV mode later on route(3) in the city. The result is depicted in Fig. 7(c).

# 9. CONCLUSION

This paper investigated a driver-centric approach that enables the drivers to select the appropriate drive modes for minimizing fuel consumption. Optimization algorithms are presented to optimize drive mode selection based on trip information, and integrated with path planning to consider intermediate filling and charging stations. An online competitive algorithm is provided that requires minimal a-priori trip information. We implement our system and evaluate the results empirically on a Chevrolet Volt. We observe a significant improvement in fuel efficiency by our system. In the extended paper [3], we generalize the online algorithm to consider four generic drive modes.

## Acknowledgement

We thank Prof. Srinivasan Keshav for helpful discussion.

# 10. REFERENCES

[1] EPA Urban Dynamometer Driving Schedule. http://www3.epa.gov/otaq/standards/light-duty/udds.htm.

[2] A. Borodin and R. El-Yaniv. *Online Computation and Competitive Analysis*. Cambridge University Press, 1998.

[3] C.-K. Chau, K. Elbassioni, and C.-M. Tseng. Drive mode optimization and path planning for plug-in hybrid electric vehicles. Technical report, Masdar Institute, 2016.

[4] Q. Gong, Y. Li, and Z.-R. Peng. Trip-based optimal power management of plug-in hybrid electric vehicles. *IEEE Transactions on Vehicular Technology*, 57:3393–3401, 2008.

[5] T. Hofman and M. Steinbuch. Rule-based energy management strategies for hybrid vehicles. *International Journal of Electric and Hybrid Vehicles*, 1:71–94, 2007.

[6] C. Hou, M. Ouyang, L. Xu, and H. Wang. Approximate pontryagin's minimum principle applied to the energy management of plug-in hybrid electric vehicles. *Applied Energy*, 115:174–189, 2014.

[7] J. Kessels, M. Koot, van den Bosch, and D. Kok. Online energy management for hybrid electric vehicles. *IEEE Transactions on Vehicular Technology*, 57:3428–3440, 2008.

[8] S. Khuller, A. Malekian, and J. Mestre. To fill or not to fill: The gas station problem. *ACM Transactions on Algorithms*, 7:534–545, 2011.

[9] E. Kim, J. Lee, and K. G. Shin. Real-time prediction of battery power requirements for electric vehicles. In *Proc. of International Conference on Cyber-Physical Systems*, 2013.

[10] N. Kim, S. W. Cha, and H. Peng. Optimal equivalent fuel consumption for hybrid electric vehicles. *IEEE Transactions on Control Systems Technology*, 20:817–825, 2012.

[11] K. Kraschl-Hirschmann and M. Fellendorf. Estimating energy consumption for routing algorithms. In *IEEE Intelligent Vehicles Symposium*, 2012.

[12] B. Mak, M. Chen, G. Zhang, L. Huang, and H. Zeng. Online energy management strategy for hybrid electric vehicle. In *ACM International Conference on Future Energy Systems (e-Energy)*, 2015.

[13] F. Mapelli, M. Mauri, and D. Tarsitano. Energy control strategies comparison for a city car plug-in hev. In *IEEE Industrial Electronics Annual Conference*, 2009.

[14] C. Musardo, G. Rizzoni, and B. Staccia. A-ECMS: An adaptive algorithm for hybrid electric vehicle energy management. In *IEEE Conference on Decision and Control*, 2005.

[15] J. A. Oliva, C. Weihrauch, and T. Bertram. A model-based approach for predicting the remaining driving range in electric vehicles. In *IEEE International Conference on Prognostics and Health Management*, 2013.

[16] S. Pourazarm, C. Cassandras, and A. Malikopoulos. Optimal routing of electric vehicles in networks with charging nodes: A dynamic programming approach. In *IEEE Electric Vehicle Conference (IEVC)*, 2014.

[17] C.-M. Tseng and C.-K. Chau. Personalized prediction of driving energy consumption based on participatory sensing. Technical report, Masdar Institute, 2016.

[18] C.-M. Tseng, C.-K. Chau, S. Dsouza, and E. Wilhelm. A participatory sensing approach for personalized distance-to-empty prediction and green telematics. In *ACM International Conference on Future Energy Systems (e-Energy)*, 2015.

[19] C.-M. Tseng, S. Dsouza, and C.-K. Chau. A social approach for predicting distance-to-empty in vehicles. In *ACM International Conference on Future Energy Systems (e-Energy)*, 2014.

[20] C.-M. Tseng, W. Zhou, M. A. Hashmi, C.-K. Chau, S. G. Song, and E. Wilhelm. Data extraction from electric vehicles through OBD and application of carbon footprint evaluation. In *ACM Workshop on Electric Vehicle Systems, Data and Applications (EV-Sys)*, 2016.

[21] T. Wang, C. G. Cassandras, and S. Pourazarm. Energy-aware vehicle routing in networks with charging nodes. In *World Congress of the International Federation of Automatic Control*, 2014.

[22] E. Wilhelm, J. Siegel, S. Mayer, L. Sadamori, S. Dsouza, C.-K. Chau, and S. Sarma. CloudThink: A scalable secure platform for mirroring transportation systems in the cloud. *Transport*, 30(3), 2015.